Received: 27 February 2020 | Revised: 29 July 2020 | Accepted: 30 July 2020 | Published on: 15 August 2020

DOI: 10.1002/joc.6782

RESEARCH ARTICLE

International Journal of Climatology | RMetS

Regional atmospheric response to the Benguela Niñas

Shunya Koseki[1,2] | **Rodrigue Anicet Imbol Koungue**[3]

[1]Geophysical Institute, University of Bergen, Bergen, Norway

[2]Bjerknes Centre for Climate Research, Bergen, Norway

[3]GEOMAR Helmholtz Centre for Ocean Research Kiel, Kiel, Germany

Correspondence
Shunya Koseki, Geophysical Institute, University of Bergen, Allégate 70, Bergen 5007, Norway.
Email: shunya.koseki@gfi.uib.no

Funding information
BANINO, Grant/Award Number: 03F0795A; Norwegian High-Performance Computing Program, Grant/Award Number: NS9039K; TRIATLAS, Grant/Award Number: 817578

Abstract

We investigate how the atmosphere is affected by the cold sea surface temperature (SST) anomalies of the Benguela Niñas using reanalysis data and a high-resolution atmospheric model. A composite analysis of reanalysis data based on five Benguela Niña events (5 years out of 39 years for 1979–2017) reveals that the rainfall along the Angolan coast is reduced significantly and other anomalies of precipitation are detected over the African continent and equatorial Atlantic. Those anomalies can be explained by the anomalies of vertically-integrated moisture flux (VIMF) and its divergence and convergence. Additionally, the Namibian low-level cloud and sea level pressure (SLP) are enhanced around the ABFZ by the Benguela Niñas. A simulation of the model forced by the cold SST anomalies of the Benguela Niñas reproduces the reduction (enhancement) of rainfall and VIMF divergent (convergent) anomaly over the Angolan coastal region (Gulf of Guinea). However, the other anomalies over the African continent are not significant. It is suggested that the effects of the Benguela Niñas are limited along southwestern coast of Africa. Composite analysis of reanalyses of rainfall anomalies associated with Benguela Niña events shows pattern over the other regions which might be induced by larger-scale atmospheric anomaly. This large-scale atmospheric anomaly can be linked with the South Atlantic Anticyclone and/or forced by the teleconnection from the tropical Pacific, for instance. The increment of the Namibian low-level cloud and SLP is simulated by the numerical experiments consistently. The low-level cloud becomes more frequent between 950 and 900 hPa and the radiative cooling by longwave radiation is reinforced during the Benguela Niñas events. In contrast, the cloud formation around 850 hPa is reduced and radiative cooling is weakened. It is indicated that this change in the cooling rate possibly induces the strengthening in the inversion layer over the cold SST anomalies.

1 | INTRODUCTION

The Angola-Benguela Frontal Zone (ABFZ) is one of remarkable characteristics in the Tropical and south Atlantic Ocean dividing the tropical warm water associated with the warm poleward-flowing Angola Current (e.g., Kopte *et al*., 2017) and subtropical cold water due to the equatorward-flowing Benguela current and coastal

upwelling system (e.g., Mohrholz *et al*., 2004; Junker *et al*., 2015; Tchipalanga *et al*., 2018; Vizy *et al*., 2018; Koseki *et al*., 2019; Siegfried *et al*., 2019). In particular, the ABFZ plays a vital role for the regional/local marine ecosystem and fishery resources (e.g., Auel and Verheye, 2007; Chavez and Messié, 2009; Jarre *et al*., 2015) providing the enriched nutrient from the sub-surface ocean to the ocean surface. Such eastern boundary ocean front system/coastal upwelling is observed ubiquitously in the global ocean, for instance, Senegal-Mauritania (North Atlantic), off California (North Pacific), and Ningaloo coast (South Indian Ocean).

Another characteristic of the ABFZ are its inter-annual variability in sea surface temperature (SST), so-called Benguela Niño/Niña (e.g., Imbol Koungue *et al*., 2017, 2019; Rouault *et al*., 2018). The peak of the amplitude of a Benguela Niño/Niña event occurs usually during February–April (e.g., Cabos *et al*., 2019; Imbol Koungue *et al*., 2019). Its horizontal distribution is, in general, limited only in the Angolan and Namibian coast. Many previous studies have shown a tight connection between Benguela Niños/Niñas and Atlantic Niños/Niñas, which are more widely-spreading SST anomalies in the tropical Atlantic Ocean, well-known as Atlantic zonal mode (e.g., Lübbecke *et al*., 2010; Jouanno *et al*., 2017; Dippe *et al*., 2018; Cabos *et al*., 2019). For instance, Lübbecke *et al*. (2010) suggested that the Benguela modes lead the Atlantic modes by approximately 3 months and those two modes seem to be bridged by the Southern Atlantic Anticyclone (SAA). Additionally, these zonal wind stress anomalies induce the downwelling/upwelling anomalies and the resulting Bjerknes Feedback (e.g., Bjerknes, 1969; Keenlyside and Latif, 2007; Cabos *et al*., 2019) enhances the SST anomalies of the Atlantic Niño/Niña in boreal summer in the equatorial Atlantic. On the other hand, the downwelling/upwelling anomalies travel eastward and southward via equatorial and coastal Kelvin waves and the anomalies outcrop in the ABFZ resulting in the Benguela Niño/Niña (e.g., Imbol Koungue *et al*., 2017, 2019; Illig *et al*., 2018; Bachelèlery *et al*., 2019). Apart from these remote dynamics of the Benguela Niño/Niña via the SAA, the Benguela mode can be also generated locally by the SAA variability (e.g., Richter *et al*., 2010). Over the ABFZ, the low-level jet associated with the SAA is prevailing (e.g., Lima *et al*., 2019) and responsible for the generation and maintenance of the Benguela coastal upwelling system. Colberg and Reason (2006) showed that the location and intensity of the ABFZ are quite sensitive to the local wind stress.

Such variability observed in the ABFZ region influences vitally the local and regional atmosphere. Using observational data, Rouault *et al*. (2003) have shown that the extreme warm events in the ABFZ induce the enhanced precipitation along the African coast. The warm events reinforce the local evaporation and cumulus convection resulting in the active precipitation over the coastal southwestern Africa. Hanshingo and Reason (2009) using idealized numerical simulations, also suggested that the warm SST anomalies modulate the moisture flux at lower troposphere and influence the rainfall activity over southwestern Africa. Apart from the local impact of the Benguela variability, Manhique *et al*. (2015) suggested that the positive SST anomalies occurring off Angola/northern Namibia fuels the moisture to eastern South Africa through the anomalous moisture flux at lower troposphere and contributes to enhance the meso-scale convective rainfall in January 2013. However, most of the studies focusing on the impacts of the Benguela variability on the regional atmospheric circulation have been performed only in the case of Benguela Niño. To our knowledge, there is no study investigating the atmospheric signature of the Benguela Niña in this region. Lutz *et al*. (2015) have performed a canonical correlation analysis based on the Atlantic Niño and Niña cases. They suggested that it is of importance to investigate how the cold SST anomalies affect the regional climate since the economy and society of western Africa highly depend on the rain-fed agriculture. The cold SST anomalies can reduce the rainfall activity inducing possibly the disastrous drought in western Africa. Therefore, in this study, we explore the impacts of the extreme cold SST events occurring in boreal spring (March–April) in the ABFZ on the regional climate using high-resolution reanalysis data and an Atmospheric General Circulation Model (AGCM). Especially, it will be investigated in what spatial scale the local SST anomaly influences the atmosphere.

The rest of this paper is structured as follows. Section 2 gives the details of data, model and methodology of analyses and simulation employed in this study. In Section 3, we will show the climatological aspects of reanalyses and model simulation. Section 4 provides the results of composite analysis of reanalysis data based on extreme cases of the Benguela Niñas. In Section 5, the results of simulations of the high-resolution atmospheric model will be given. Finally, in Section 6, we will summarize this study with discussions.

2 | DATA, MODEL, AND METHODOLOGY

In this study, we use the reanalysis data of ERA-Interim (Dee *et al*., 2011) and ERA5 (Copernicus Climate Change Service, 2017) to investigate the atmospheric responses to the Benguela Niñas in March and April. Both data have a horizontal resolution of 0.25° covering 39 years from 1979 to 2017, but the ERA-Interim is interpolated grid from original 0.75° at the European Centre for Medium-Range Weather Forcasts website (https://www.ecmwf.int/en/forecasts/datasets/reanalysis-datasets/era-interim). Using those reanalysis data, a composite analysis is carried out based on the Benguela Niña events. Many of previous studies have detected the Benguela Niño/Niña events (e.g., Florenchie *et al*., 2003; Rouault *et al*., 2007). Recently, Imbol Koungue *et al*. (2019) defined the Benguela Niños/Niñas comprehensively using a combination of observational and satellite data. According to Imbol Koungue *et al*. (2019), the extreme Benguela Niñas in boreal spring (February–April) have occurred in 1982, 1985, 1992, and 1997 from 1958 to 2015 period. In this study, the relatively strong cold event in 1983 (see fig. 3 in Imbol Koungue *et al*., 2019) is also considered and the composite analysis based on five strong Benguela Niña events is performed for ERA-Interim and ERA5 reanalyses. To have more robust results, we use the two different reanalysis data set in this study.

Figure 1 gives the composite of SST anomalies of the five Benguela Niña events in March–April obtained from ERA-Interim (hereafter, composite anomaly) and defined as anomaly from March to April mean climatology (we have confirmed that the SST anomaly due to the Benguela Niñas is quite similar between ERA-Interim and ERA5, not shown). This method will be performed for each variable. The strong cold SST anomaly is confined in the ABFZ with amplitude of about −2.4 K. Moreover, the cold anomalies spread over the South Atlantic and Agulhas Retroflection Current as well. In particular, the anomaly in the South Atlantic seems to be related to the SAA variability (it will be shown later). In March–April, the SST anomaly is much weaker in the equatorial Atlantic indicating that the Benguela Niño/Niña leads the equatorial Atlantic Niño/Niña by a few months (e.g., Lübbecke *et al*., 2010; Cabos *et al*., 2019; Imbol Koungue *et al*., 2019; Keenlyside et al., 2020). In the global scale, there is no outstanding SST anomalies observed in this composite analysis in March–April except for the narrow band of warm SST along the Peruvian coast and the moderate warm SST anomalies in the tropical Pacific (even though they are not statistically significant at 90%) in Figure 1. This warm SST anomaly in the tropical Pacific is residual of the warm SST anomaly in January (up to 2 K) indicating the possibility of inter-basin teleconnection between two basins (e.g., Cai *et al*., 2019). But, the teleconnection between the Pacific and Atlantic basin is beyond the scope of this study.

Because the Benguela Niñas tends to be connected with the SAA and equatorial Atlantic variabilities (e.g., Lübbecke *et al*., 2010; Lutz *et al*., 2015; Cabos *et al*., 2019), the results of composite analysis with reanalyses can be also influenced by those variabilities. In order to subtract the 'pure' impacts of the Benguela Niñas on the atmosphere, a numerical simulation is also carried out in a similar way to Hanshingo and Reason (2009). The Community Atmospheric Model version 5.0 (CAM5, Neale *et al*., 2010) coupled with the Community Land Model (CLM) with high-resolution

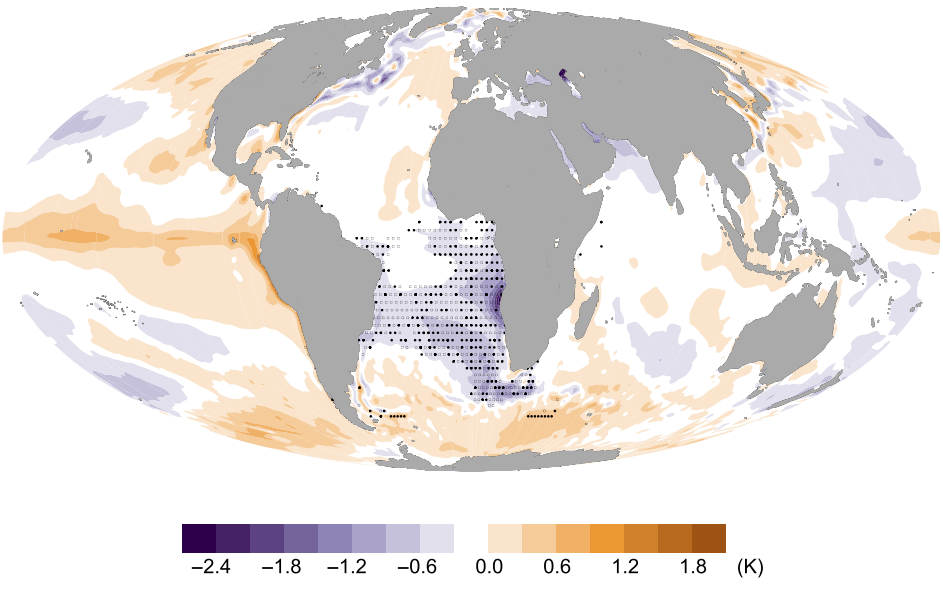

FIGURE 1 Composited March–April SST anomalies of ERA-interim in the five events defined in Imbol Koungue *et al*. (2019) for 1982, 1983, 1985, 1992, and 1997. Black dots denote the significance level of 90%

configuration is employed for the numerical simulations. CAM5 in this study has a spatial resolution of 0.23° × 0.31° with 30 vertical layers. Initialized by climatological state and forced by climatological SST obtained from Hadley Centre Sea Ice and Sea Surface Temperature (HadISST, Rayner *et al*., 2003) data set, 1-year spin-up is conducted. After the spin-up, two different semi-idealized experiments are demonstrated. One is control run (CTL) and integrated for 4 months (January–April) forced by the climatological SST obtained from HadISST. Other is Benguela Niña run (NINA) implemented for 4 months and forced by climatological SST with the composited SST anomaly of the Benguela Niña SST from ERA-Interim in the ABFZ. The SST composite anomalies are estimated from January to April for the selected event year (Figure 4). Note that any positive SST anomalies for the SST boundary condition are set to zero because this study focuses on the cold SST events. But, the warm SST anomalies are only seen in January composite around the ABFZ. Both simulations contain 30 ensemble members fluctuated by $O(10^{-10})$ of atmospheric temperature noise in the initial condition of one-year spin-up. In this study, all of the statistical significance for anomaly fields is based on Student's *t*-test methodology.

3 | CLIMATOLOGY

Figure 2 summarizes the March–April climatology of ERA-Interim and CAM_CTL ensemble mean for different parameters. In March–April as shown in Figure 2a, the tropical rainband associated with the Inter-tropical Convergence Zone (ITCZ) is located at the equator and south of the equator. Over the African continent, the intense precipitation concentrates over the Congo Basin spreading to the Mozambique Channel and Madagascar. Along the Angolan and Namibian coastline, there is a transition zone from rainy to arid regions (in particular, April is the rainy season in Angola). Off Angola-Namibia coastal zone, the precipitation is largely suppressed, associated with the cold SST due to the Benguela upwelling and the subsidence due to the SAA system. This distribution of climatological precipitation can be characterized by the vertically-integrated moisture flux (VIMF) from the surface to the top of atmosphere of the system and its divergence in Figure 2c. Over the tropical and south Atlantic, a basin-scale anti-clockwise circulation of VIMF is dominant. Moreover, the ITCZ and vigorous terrestrial rainfall are well consistent with the VIMF convergence and subtropical ocean is with the divergence. Conversely, less precipitation over the subtropical Atlantic is associated with the VIMF divergence. While the subtropical Atlantic is covered by frequent maritime low-level cloud (e.g., Richter and Mechoso, 2004; Potter *et al*., 2017), the equator is almost low-level cloud free in Figure 2e. Such low-level cloud deck is indicative for inhibition of cumulus convection, underlying cool SST and the SAA shown in Figure 2g. We have also browsed images (https://isccp.giss.nasa.gov/)) of the observed data of low-level cloud amount of the International Satellite Cloud Climatology Project (ISCCP, Schiffer and Rossow, 1983, not shown). We have found that ERA-interim and ERA5 represent the distribution and amount of low-level cloud over the southeastern Atlantic well. The SAA is centred around 0°E and 33°S and the intense south-easterly is prevailing along the Angolan-Namibian coast (e.g., Lima *et al*., 2019). Although the precipitation in the ITCZ and over the Congo Basin is over- and underestimated respectively, the simulated precipitation and VIMF in CAM_CTL agree very well with the ERA-Interim (Figure 2b,d). The distribution of the low-level cloud in CAM_CTL also captures the Namibian cloud deck consistently (Figure 2f). In Figure 2h, the location of the core of the SAA and the associated coastal low-level jet are also simulated quite reasonably. Especially, the wind stress over the ABFZ simulated by the high resolution CAM5 is highly realistic while the low resolution of CAM4 shows the erroneous wind stress over the ABFZ, which is one of causes for the warm SST biases in earth system models (Xu *et al*., 2014; Koseki *et al*., 2018; Voldoire *et al*., 2019). Figure S1 summarizes the climatology of ERA5 for 1979–2017 and there is a good agreement with ERA-Interim and CAM_CTL.

4 | COMPOSITE ANALYSIS OF ERA-INTERIM AND ERA5

In this section, we investigate how the regional atmosphere can be influenced by the Benguela Niñas in March–April based on composite analysis of ERA-Interim and ERA5. The aforementioned climatological features are modified by the Benguela Niñas shown in Figure 3. The precipitation is significantly suppressed around the coasts of Angola and Namibia in Figure 3a, which is opposite to the cases of Benguela Niños (e.g., Rouault *et al*., 2003). While it is expected that such negative anomaly of coastal precipitation is induced by the cold SST events according to Lutz *et al*. (2015), there are other anomalies of the precipitation found over/around the African continent: the precipitation is enhanced to some extent over the Congo Basin and suppressed around the East African Great Lakes (Lakes Victoria, Malawi, and Tanganyika) with some significance. The other positive anomaly of the rainfall with significance is found off eastern South Africa around

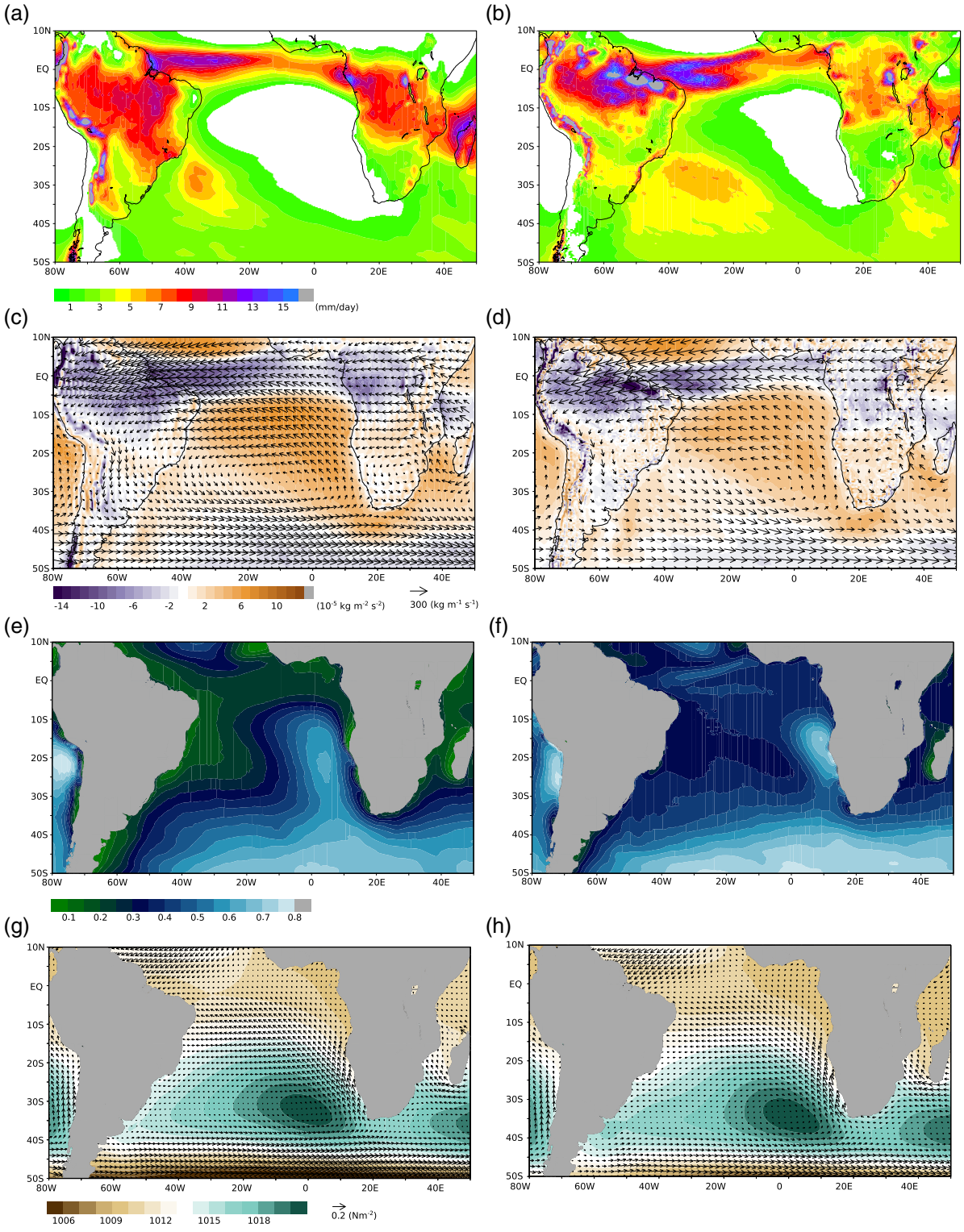

FIGURE 2 (Left) March–April climatology of ERA-interim for 1979–2016 and (right) 30 ensemble means of CAM_CTL for (first row) precipitation, (second row) vertically-integrated moisture flux (arrows) and its divergence (colour), (third row) low-level cloud fraction and (fourth row) sea-level pressure (colour) and wind stress (arrows), respectively

30°E–40°E and 40°S–35°S. Moreover, the rainfall associated with the ITCZ is also modulated in the composite of the strong Benguela Niñas indicating a meridional change in the ITCZ. Those precipitation anomalies have a good agreement with the anomalies of VIMF and its divergence as shown in Figure 3c. Interestingly, an anticlockwise VIMF anomaly is detected over the ABFZ and the moisture seems to be removed effectively over the

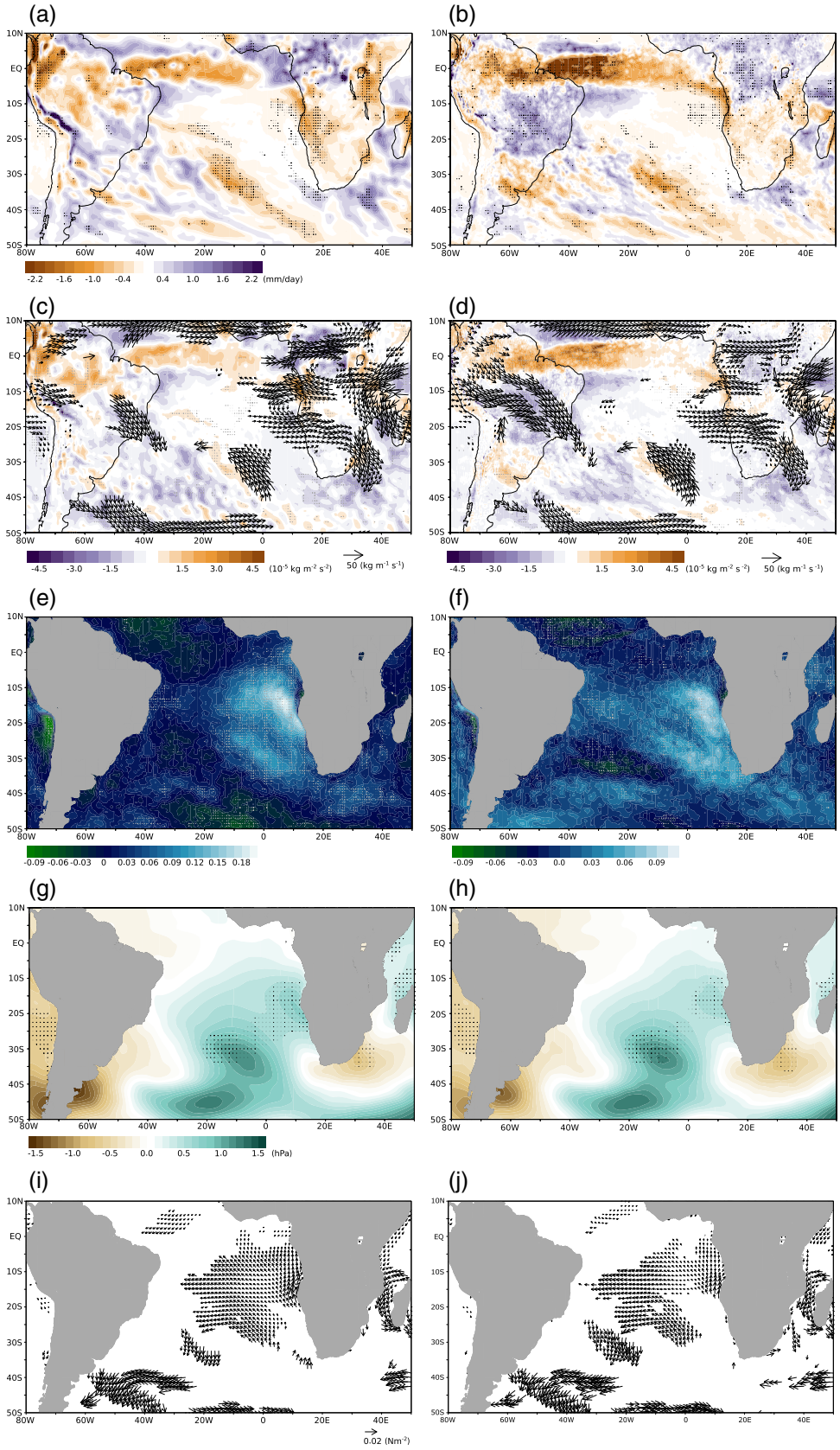

FIGURE 3 Composited March–April anomalies of (left) ERA-interim (right) ERA5 in the five events of the Benguela Niñas for (top) total precipitation, (middle) vertically-integrated moisture flux and its divergence, and (bottom) low-level cloud. The dots denote the significance level of 90% and arrows in Figure 3c,d show only significance anomalies with 90%. For (top) sea level pressure and (bottom) wind stress. The dots denote the significance level of 90% and arrows in Figure 3i,j show only significance anomalies with 90%

Angolan coastal region resulting in the VIMF divergence anomaly there. This anti-clockwise VIMF anomaly, inversely, seems to bring more moisture (via Namibia and Botswana) toward eastern South Africa where the convergence is enhanced and the precipitation is amplified at the coast (Figure 3a). A similar remote impact of the Benguela variability on eastern South Africa has been discussed in Manhique *et al.* (2015). However, in their

case of the Benguela Niño (warm SST) event in January 2013, the eastward VIMF anomaly flows through a different pathway over Angola, Zambia, Zimbabwe, and Mozambique toward eastern South Africa corresponding to the cyclonic anomaly of VIMF over the ABFZ (see fig. 6 of Manhique *et al*., 2015). To the north of the ABFZ, a cyclonic anomaly of VIMF is found over the Congo Basin. The north branch of the cyclonic flow can transport more moisture from the equatorial Atlantic to the Congo Basin and consequently, the VIMF convergence is enhanced. The convergence is attributable for the enhanced precipitation over the Congo Basin (Figure 3a). To the east of the Congo Basin, the divergence anomaly of VIMF is found and consistent with the dry anomaly around the east African Great Lakes (Figure 3a). However, the divergence anomaly here seems to be more relevant to the VIMF anti-cyclonic anomaly over the Mozambique Channel and Madagascar (even though the composite SST anomalies in the Indian Ocean is quite small in Figure 1). In the warm SST case, the cyclonic anomaly of the moisture flux at 850 hPa is induced around Madagascar (see Figure 4 in Hanshingo and Reason, 2009). With the numerical experiments, we will also investigate if such convergence and divergence anomalies far from around the ABFZ can be induced by the Benguela Niñas in the next section.

The marine low-level cloud forms more frequently (up to 0.17) around the ABFZ shown in Figure 3e. As the VIMF anomaly indicates, the Benguela Niña can generate anti-cyclonic circulation locally over the ABFZ. In addition, the cold SST anomaly is favourable condition for the marine low-level cloud formation as well. These situations can be explainable for the frequent cloud formation. The enhancement of low cloud formation extends widely to the central part of the South Atlantic Ocean (around 0°E). We will survey how important the localized cold SST in the ABFZ is for the low-level cloud formation in the next section. The SAA is centred at 0°E and 35°S (Figure 2g) and is excited in the case of Benguela Niñas (Figure 3g) by 1.0 hPa. As suggested by previous studies (e.g., Lübbecke *et al*., 2010; Richter *et al*., 2010; Cabos *et al*., 2019), the Benguela variability is connected well with the SAA variability. Interestingly, the SLP seems to be reinforced locally over the ABFZ with a smaller amplitude (about 0.5 hPa, Figure 3g). This local high-pressure anomaly can be explainable for the anti-clockwise anomaly of VIMF and the more frequent low-level cloud in Figure 3c,e. In the case of the Benguela Niñas, the southeasterly anomaly tends to be reinforced and in particular, the coastal low-level jet (e.g., Lima *et al*., 2019) is enhanced in Figure 3i. The enhanced coastal low-level jet could be a cause to amplify the coastal upwelling resulting in the Benguela Niñas. However, the wind stress does not show the local anti-cyclonic flow around the ABFZ clearly while the wind stress anomaly is anti-cyclonic around Madagascar, which is consistent with the VIMF anomaly in Figure 3c.

In principle, the patterns of the atmospheric variable anomalies of ERA5 are quite similar to those of the ERA-Interim. Inversely, the reduction of Angolan precipitation

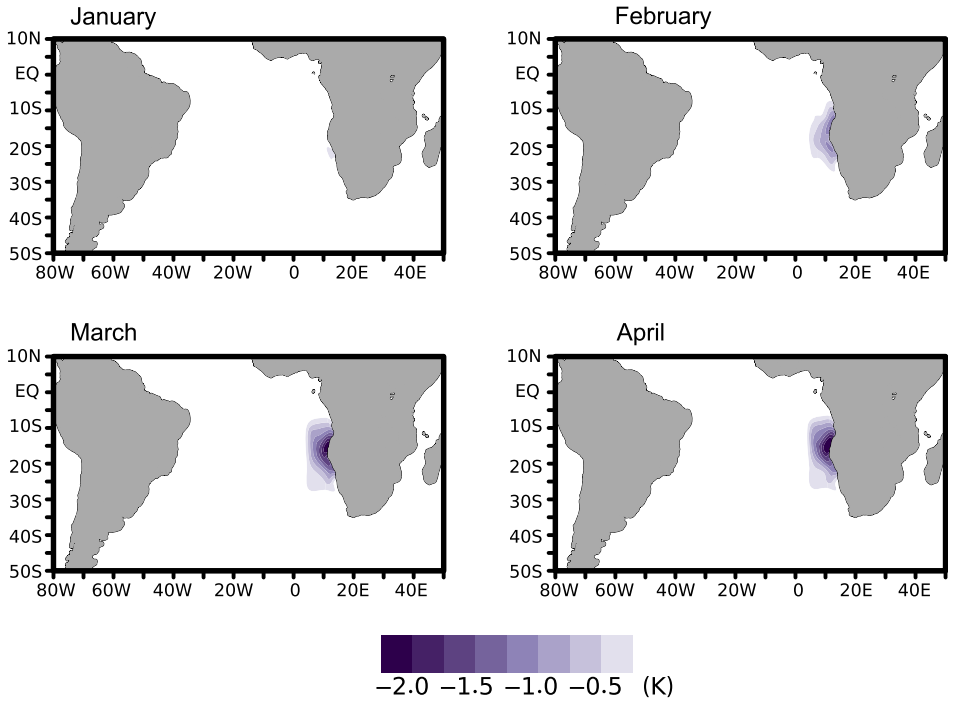

FIGURE 4 SST anomalies in the ABFZ added on the SST boundary condition for CAM_NINA

is more constrained around the coastal area and dry anomaly over the ocean is extended more equatorward from the western African coast in Figure 3b. The enhancement in precipitation over the Congo Basin is slightly less in ERA5 than in ERA-Interim (Figure 3a,b), but relatively more significant. Although the dry anomaly around the East African Great Lakes are smaller in ERA5 than in ERA-Interim, these patterns of rainfall anomaly over the African Continent are quite similar to those in ERA-Interim. The ITCZ anomaly is also approximately identical even though the negative anomaly is larger. In addition, the other anomalies of precipitation are also in agreement for instance, enhancement off eastern South Africa, the Congo Basin, and to the south and west of Madagascar. Figure S1 gives the composite anomaly for the extreme Benguela Niña years of the observed precipitation of the Global Precipitation Climatology Project (GPCP, Adler *et al*., 2003). The observed anomalies of precipitation are approximately identical with those in reanalysis, in ERA5: the reduced precipitation along Angola, ITCZ and around the East African Great Lakes and enhanced rainfall over the Congo Basin and off east South Africa are well consistent between GPCP and ERA5. The VIMF and its divergence anomalies around the African Continent are also approximately identical between two reanalysis products in Figure 3c,d. The Namibian low cloud deck is also enhanced locally around the ABFZ, but its amplitude is relatively modest in ERA5 (up to 0.09, Figure 3f). The amplified SAA and high-pressure anomaly around the ABFZ in ERA5 are approximately equal to those in ERA-Interim (Figure 3g,h). The significant wind stress anomaly in ERA5 is also quite similar to that in ERA-Interim in Figure 3i,j indicating a relationship between Benguela Niña and enhanced SAA.

5 | SEMI-IDEALIZED SIMULATION OF HIGH-RESOLUTION CAM5

In the preceding section, the composite analysis suggests that the Benguela Niñas influence the regional atmosphere in an opposite way to the Benguela Niños (e.g., Rouault *et al*., 2003; Hanshingo and Reason, 2009). However, the composite anomalies based on the Benguela Niña events would be contaminated by other factors such as enhanced SAA. In this section, by semi-idealized experiments of a high resolution AGCM, we investigate the atmospheric responses to the localized SST cold anomaly. Aforementioned in Section 3, the simulation of CAM5_CTL is capable to reproduce the climatology realistically in this region (Figure 2).

Figure 5 summarizes the anomalies of atmospheric variables between CAM_NINA and CAM_CTL. As seen in ERA-Interim and ERA5, the localized cold SST anomaly suppresses the precipitation along the Angolan coast in CAM5 simulation (Figure 5a). Its equatorward extension seems to be more similar to that in ERA5 (Figure 3b). In contrast, the precipitation is enhanced over the Gulf of Guinea with statistical significance, which can be seen in ERA-Interim and ERA5 in Figure 3a,b (even though those anomalies are not statistically significant). Over the African Continent (in particular, the Congo Basin and East African Great Lakes), there is no significant reduction and enhancement of the precipitation and the anomalies are not as organized as ERA-Interim and ERA5. This indicates that the localized cold SST anomaly is not a main source for the anomalies of precipitation over the African Continent. Even though the positive rainfall anomaly is detected off eastern South Africa, its amplitude is relatively less. The anomaly in the ITCZ is quite noisy and differs largely from those in ERA-Interim and ERA5. Corresponding to the rainfall anomalies along Angolan coast, the VIMF divergence is enhanced (Figure 5b). To the north of the ABFZ, there is an anti-cyclonic anomaly of VIMF, which is similar to those in the reanalyses (Figure 3c,d). The VIMF divergence anomaly is also attributed to the anomalous flow of the northwestward VIMF between 5°S and the equator. This northwestward anomaly of the VIMF forms the VIMF convergence anomaly over the Gulf of Guinea and consequently, the precipitation is enhanced there (Figure 5a). Inversely, the VIMF anomaly is not significant over the African Continent compared to ERA-Interim and ERA5. Whereas the westerly anomaly of VIMF is observed over eastern South Africa to southern Madagascar, this anomaly appears not to be connected with the anti-cyclonic VIMF anomaly over the ABFZ.

Interestingly, the Namibian low-level cloud is more frequent in the case of Benguela Niñas in CAM5 simulation (Figure 5c). Its enhancement spreads only locally around the ABFZ, but its amplitude is up to 0.12 and comparable with those in ERA-interim and ERA5 (Figure 3e,f). The enhanced formation of low-level cloud can be linked with the positive anomaly of SLP around the ABFZ in CAM_NINA as shown in Figure 5d (its amplitude is up to 0.5 hPa, which is approximately identical with those in ERA-Interim and ERA5 as shown in Figure. 3g,h). This high-pressure anomaly generates the wind stress anomaly around the ABFZ: North of the ABFZ, the anomaly is southerly or southeasterly divergent flow and the background southerly surface wind is strengthened. South of the ABFZ, the wind stress

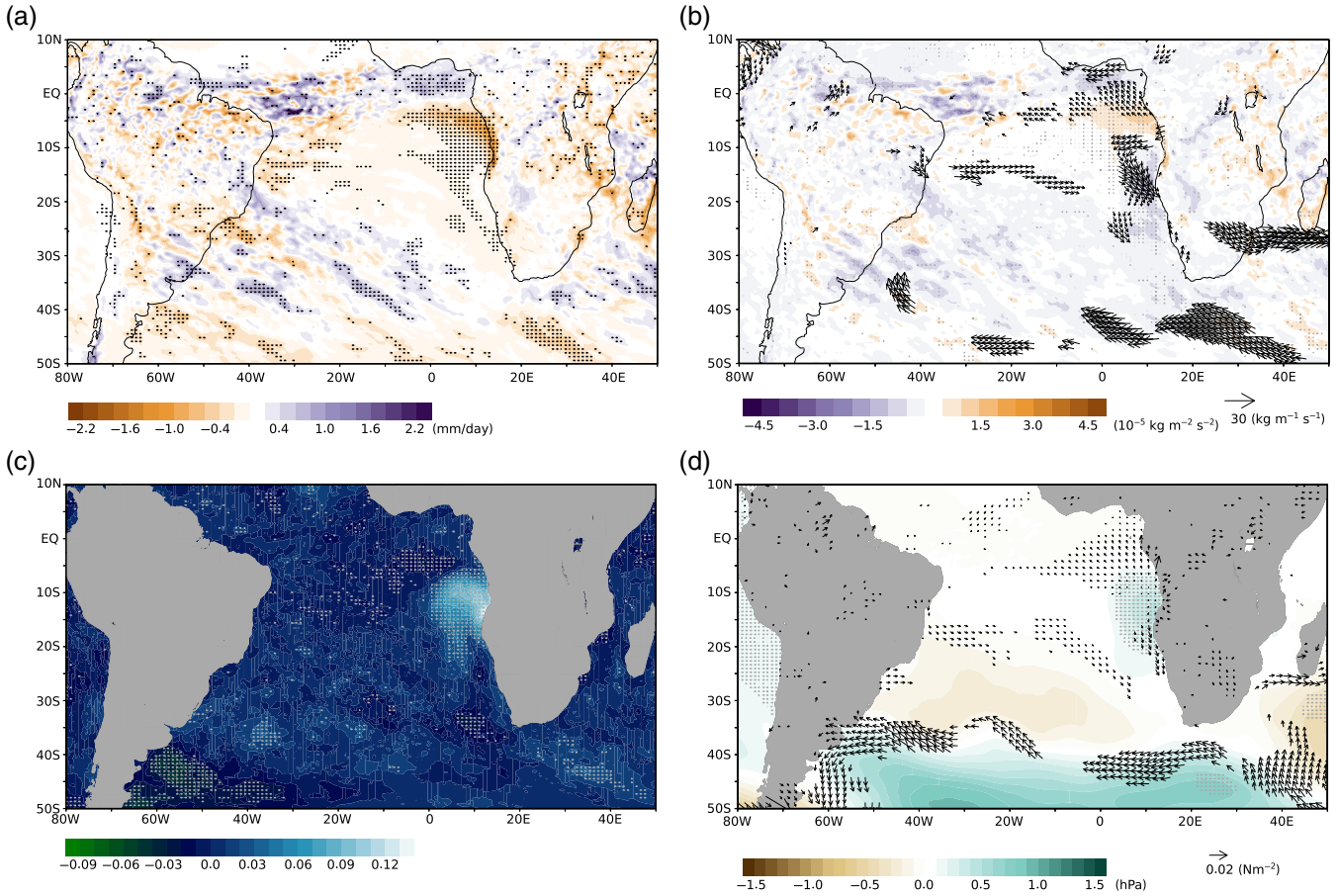

FIGURE 5 March–April anomalies between CAM_NINA and CAM_CTL of (a) total precipitation, (b) vertical-integrated moisture flux (arrows) and its divergence (colour), (c) low-level cloud fraction, (d) sea level pressure (colour) and wind stress (arrows). Dots denote the significance level of 90%. Vectors show only the anomalies with the significance level of 90%

anomaly is northerly along the coast, which might tend to diminish the coastal low-level jet. These results suggest that the local cold SST anomalies associated with the Benguela Niña tends to enhance the contrast between the tropical Atlantic (ITCZ and vigorous precipitation around the equator) and subtropical South Atlantic (high pressure, less precipitation, and low-level cloud deck) South Atlantic, at least, along the west African coast. This change in low-level cloud formation can be also discussed more insightfully by low-level atmospheric static stability, Γ, (e.g., Klein and Hartman, 1993) determined by,

$$\Gamma = \theta_{700\,\mathrm{hPa}} - \theta_{1{,}000\,\mathrm{hPa}}$$

where θ is the potential temperature at 700 and 1,000 hPa. Note that in this study we use the potential temperature at 690 and 992 hPa instead, which are the pressure levels of the default configuration of CAM5. Figure 6 gives the ensemble mean static stability in CAM_CTL and its difference between CAM_NINA and CAM_CTL. CAM_CTL is able to represent the strong stability in the subtropical Atlantic well (Figure 6a), which is a good agreement with Klein and Hartmann (1993). Benguela Niña event strengthens the static stability locally by about 2 K as shown in Figure 6b. Klein and Hartmann (1993) regressed the cloud amount on the stability and found the value of 5.70 (% per K; see fig. 13 of Klein and Hartmann, 1993). Our results show that the static stability becomes stronger by 2 K and low-level cloud formation is more frequent by 0.12 (equal to 12%), meaning that the enhanced cloud formation is linked tightly to the reinforced stability in agreement with Klein and Hartmann (1993) even though they estimated it by annual mean value.

Another important aspect of low-cloud-covered atmosphere is inversion layer (e.g., Hess, 2004) and it is of interest to see how the Benguela Niña event modulates it. Figures 7a–c illustrate the vertical profiles of temperature, cloud fraction, and heating rate due to longwave radiation in CAM_CTL averaged over 16°S–11°S and

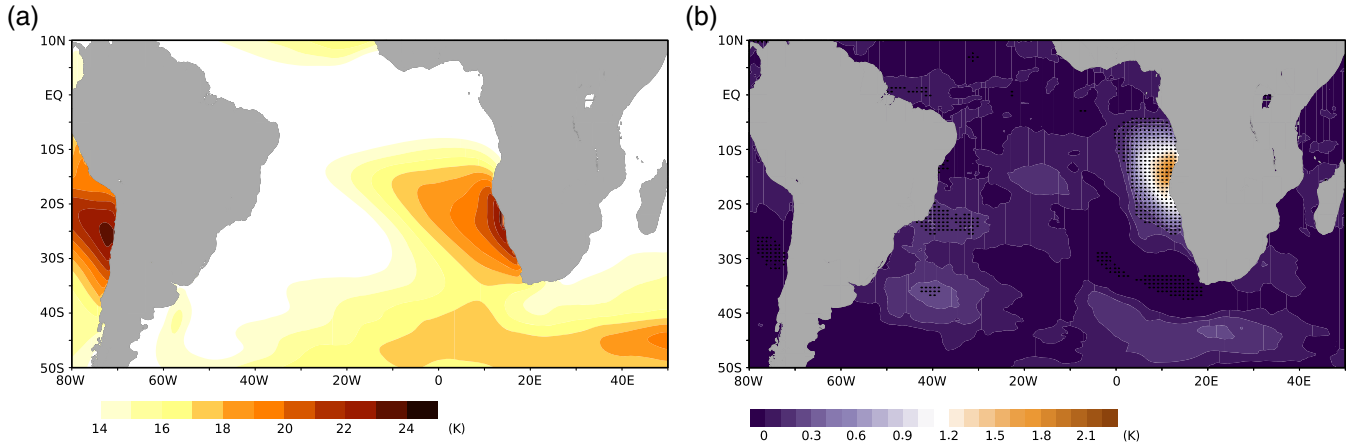

FIGURE 6 (a) March–April ensemble mean low-level static stability of CAM_CTL and (b) its anomaly between CAM_NINA and CAM_CTL. Dots denote the significance level of 90%

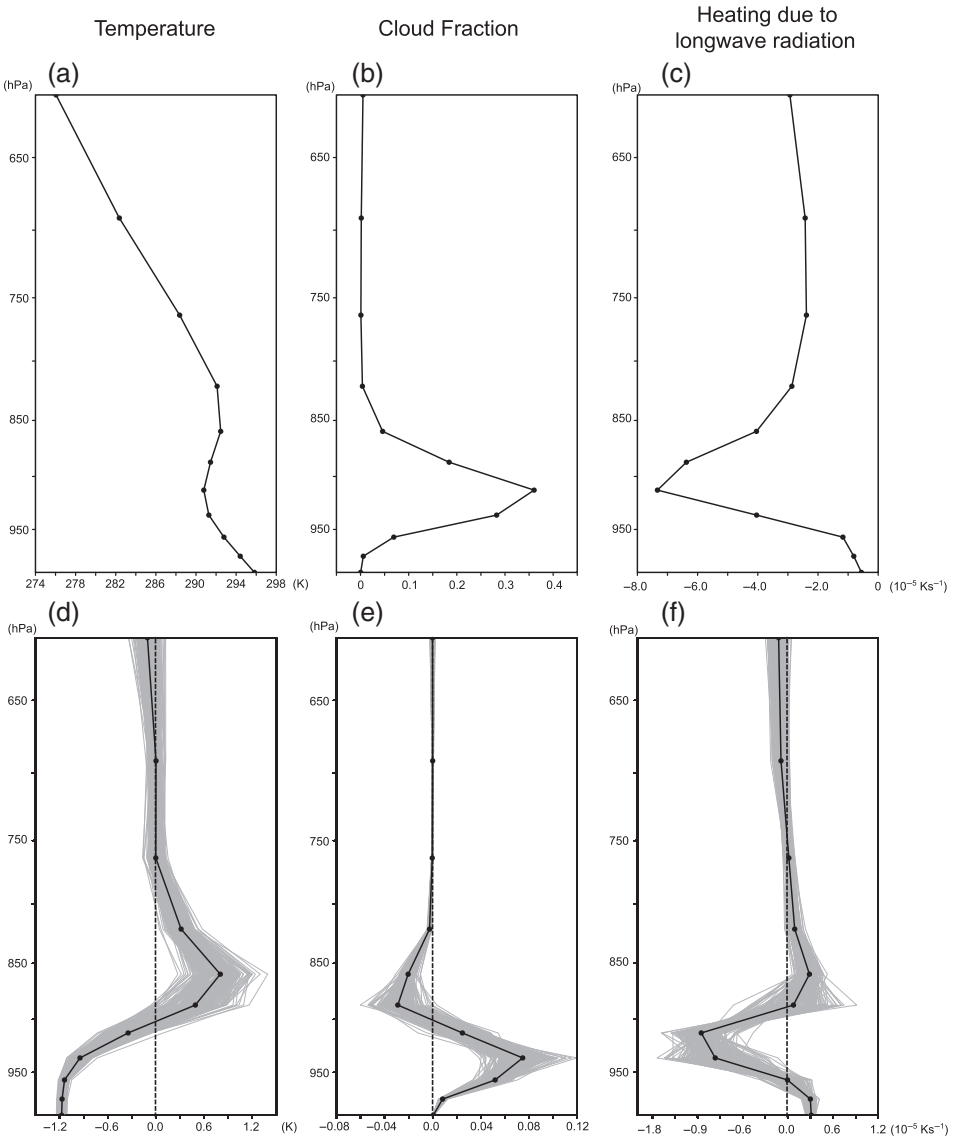

FIGURE 7 (a–c) Thirty ensemble mean of vertical profiles of temperature, cloud fraction, and heating due to longwave radiation in CAM_CTL averaged over 5°E–10°E and 16°S–11°S. (d–f) 30 ensemble mean difference (black) of vertical profiles of temperature, cloud fraction, and heating due to longwave radiation between CAM_NINA and CAM_CTL. Grey lines denote each resampled 15 ensemble mean difference. The resampling is repeated 200 times by Monte Carlo method

5°E–10°E. The mean vertical profile of temperature shows a weak inversion layer (about 2 K difference) between 925 and 850 hPa (Figure 7a). The subsidence associated with the high-pressure system (through adiabatic heating) also contributes to form the inversion layer which can inhibit the atmospheric convection or block atmospheric flow. Consequently, the precipitation is suppressed (see Figure 2b). Around the inversion layer, cloud formation is more frequent (maximum at 900 hPa shown in Figure 7b), suggesting that it is cloud-topped boundary layer from the surface to about 900 hPa over the ABFZ. This low-level cloud induces radiative cooling due to longwave around the cloud top (e.g., Nicholls, 1984; Koračin *et al*., 2005; Koseki *et al*., 2012; Wood, 2012; Kato *et al*., 2018) as seen in Figure 7c. With the presence of cold SST anomalies in the ABFZ, the inversion layer is strengthened by cooling below 900 hPa and warming around 850 hPa in Figure 7d (Note that the grey lines in Figure 7d–f are differences between randomly selected 15 ensemble members and this procedure is repeated 200 times). While the surface cooling is related to less sensible heat flux (see the next section), the cooling around 950–900 hPa and warming at 850 hPa can be attributed to the modulation of cloud formation as seen in Figure 7e,f: the low cloud is enhanced between 950 and 900 hPa and slightly infrequent above 900 up to 800 hPa. The heating rate due to longwave radiation decreases and increases correspondingly. The vertical distribution of this modulation in longwave radiative heating is approximately consistent with that of temperature (Figure 7d).

6 | DISCUSSION AND CONCLUDING REMARKS

This study has investigated how the Benguela Niña SST anomalies influence the atmosphere with state-of-the-art reanalysis data and high-resolution AGCM model focusing on extreme cases of Benguela Niñas in March–April (Imbol Koungue *et al*., 2019). The composite analysis shows that the Benguela Niñas suppress the precipitation along Angolan coast, which is an opposite impact to the Benguela Niños (e.g., Rouault *et al*., 2003; Hanshingo and Reason, 2009). Not only such local rainfall, but also remote rainfall anomaly can be seen in the composite analysis: enhanced rainfall over the Congo Basin, Gulf of Guinea and off eastern South Africa and suppressed in the ITCZ and over East African Great Lakes. Those precipitation anomalies are explainable by the VIMF divergence and convergence. In particular, the anti-cyclonic VIMF anomalous flow and its divergence causes the rainfall along Angolan coast to be reduced. The semi-idealized simulation of CAM5 (CAM_NINA) also shows the reduction of coastal precipitation and anti-clockwise VIMF anomalous circulation over the ABFZ. In addition, the southeasterly VIMF anomaly contributes to the VIMF divergence along Angolan coast. The enhancement of rainfall over the Gulf of Guinea seems to be induced by the southeasterly VIMF and its convergence. However, other anomalies of precipitation are very noisy and VIMF anomaly is not significant over the African Continent in the CAM_NINA simulation.

In the composite analysis of ERA-Interim and ERA5, the atmospheric circulation can be affected by other factors such as the residual warm SST anomaly in the tropical Pacific and the strengthened SAA (Figure 1 and Figure 3g,h). For example, the ITCZ anomaly over the western equatorial Atlantic is more directly linked with the SAA anomaly through modification in the equatorial trade wind as there is a high correlation between the SAA and equatorial Atlantic variability (e.g., Lübbecke *et al*., 2010; Richter *et al*., 2010). This study suggests that the remote impacts of the Benguela variability, which Manhique *et al*. (2015) presented, might need additional atmospheric anomalous circulation and the influences of Benguela variability is restricted locally over the western African coastal region.

Both composite analyses and simulations showed that the formation of the Namibian low-level cloud is enhanced by the Benguela Niñas. Its amplifying rate agrees well with the one observed by Klein and Hartmann (1993). This increment of low-level cloud can be explained by the facilitated saturation associated with the surface cooling (e.g., Tokinaga and Xie, 2009). As Figure 8 shows, the latent and sensible heat fluxes are reduced significantly around the ABFZ (Figure 8ab) by the Benguela Niñas. In particular, the reduced sensible heat can cool the atmospheric boundary layer down and this situation is favourable for more condensation resulting in more frequent cloud fraction. Conversely, to the north of the ABFZ, the both of the fluxes are enhanced. This amplification of heat flux is induced by the stronger surface wind to the north of the ABFZ as shown in Figure 5d. This stronger southerly wind is in a good agreement with the enhanced SLP meridional gradient shown in Figure 8c. This relation between surface wind and SLP gradient invokes us the pressure adjustment mechanism by Lindzen and Nigam (1987). It is also a novel indication that the Benguela variability drives the surface wind via the pressure gradient mechanism. It will be interesting, as a future work, to perform similar simulations in the case of Benguela Niño to see how the situation is different. Moreover, this accelerated surface winds create the convergence over the Gulf of Guinea and enhanced precipitation there (Figure 6a,b). Even though

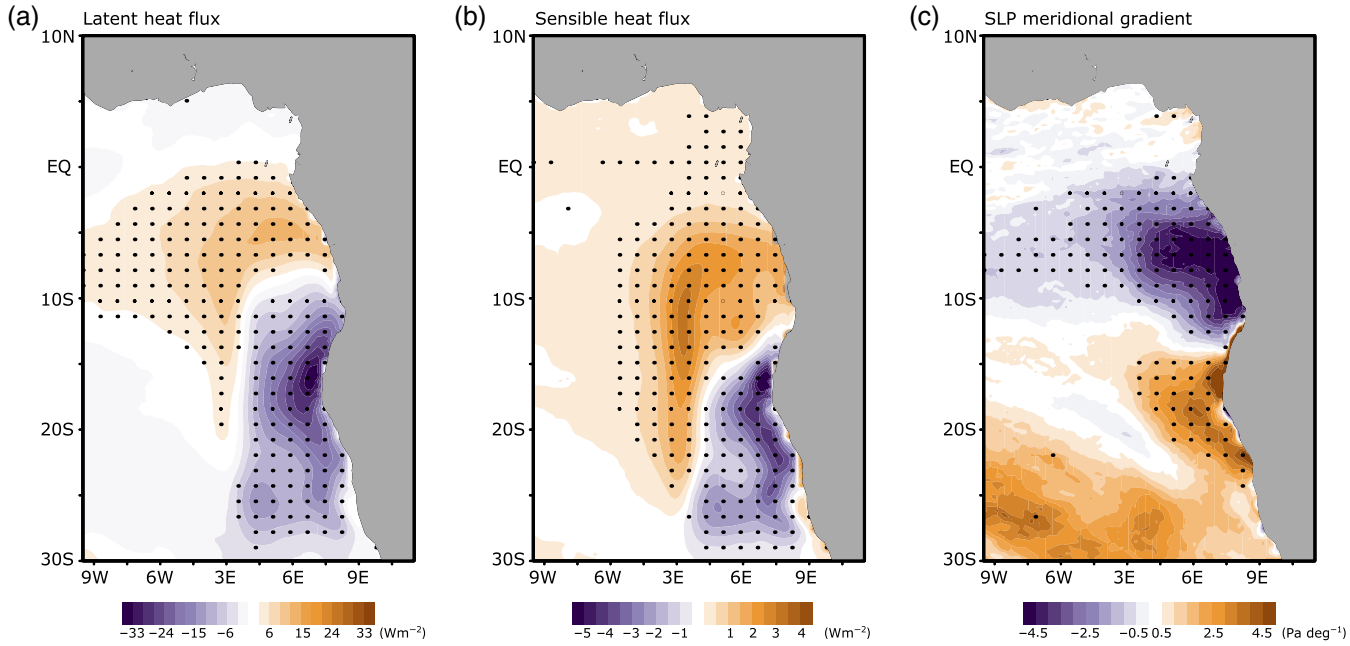

FIGURE 8 Same as in Figure 5, but for the zoomed-up (a) latent heat flux, (b) sensible heat flux, and (c) SLP meridional gradient, respectively. Upward heat fluxes are positive

the composite analysis of ERA-Interim and ERA5 also shows the enhanced precipitation over the Gulf of Guinea, the signal is not significant in the composite analysis. Possible reasons for this are because (1) there are only five cases in the composite analysis (30 ensemble members for CAM5 simulation) and (2) the precipitation variability over the Gulf of Guinea would be contaminated by the ITCZ anomaly and/or larger-scale atmospheric circulation anomaly in the composite analysis. Interestingly, the Benguela Niña strengthens the inversion layer between 950 and 850 hPa in the lower troposphere modulating the vertical profile of cloud formation. The low-level cloud tends to be more frequent in the slightly lower level (950–900 hPa) and infrequent in the upper level (850 hPa) as shown in Figure 7e. This vertical shift of cloud induces the increase and decrease of longwave radiative cooling in the lower and upper level respectively and consequently, the inversion layer becomes more stable. The vertical turbulent mixing is less effective over the cooler SST (e.g., Wallace *et al*., 1989; Tokinaga *et al*., 2006) and the atmospheric boundary layer tends to be shallow. A similar situation can explain the shallower cloud-topped boundary layer over the Benguela Niñas in our simulations and the heating distribution can be also shifted.

This study provides a first look at the impacts of the Benguela Niñas on the atmosphere and our results are novel because we suggest that the Benguela Niñas activate the low-level cloud formation for the first time. On the other hand, there are still some shortcomings of this study and necessary of further investigation: our model has a coarse vertical resolution and might be insufficient to explore the cloud-topped boundary layer. We will need a simulation with denser vertical layer in the lower troposphere. The higher local SLP induces a stronger subsidence and this also modifies the heating in the lower troposphere. Therefore, a further quantification will be necessary with a heat budget analysis to discuss the modulation in the inversion layer. Moreover, the Benguela Niñas tend to decelerate the coastal low-level jet to the south of the ABFZ. This reduction could weaken the coastal upwelling and, in that case, the Benguela Niñas could be decayed. This means that there might be a negative feedback in the Benguela Niña, which might be a counterevidence against previous studies suggesting the coastal Bjerknes Feedback (e.g., Kataoka *et al*., 2013). However, this speculation can be elucidated by an approach of coupled and ocean modellings in the future.

ACKNOWLEDGEMENT

The authors are supported by TRIATLAS, which has been received funding from the European Union's Horizon 2020 research and innovation program under grant agreement No. 817578. The authors express their appreciation to I. Bethke and M. -L. Shen who provided their technical advices and helps to conduct the simulations of high resolution CAM5. The computational resource is supported by Norwegian High-Performance Computing Program resources (NS9039K). This study was further supported by the German Federal Ministry of

Education and Research as part of the BANINO (03F0795A) project.

ORCID

Shunya Koseki https://orcid.org/0000-0001-7205-7434
Rodrigue Anicet Imbol Koungue https://orcid.org/0000-0003-1447-4226

REFERENCES

Adler, R.F., Huffman, G.J., Chang, A., Ferraro, R., Xie, P.P., Janowiak, J., Rudolf, B., Schneider, U., Curtis, S., Bolvin, D., Gruber, A., Susskind, J., Arkin, P. and Nelkin, E. (2003) The version 2 global precipitation climatology project (GPCP) monthly precipitation analysis (1979-present). *Journal of Hydrometeorology*, 4(6), 1147–1167.

Auel, H. and Verheye, H.M. (2007) Hypoxia tolerance in the copepod Calanoides carinatus and the effect of an intermediate oxygen minimum layer on copepod vertical distribution in the northern Benguela current upwelling system and the Angola-Benguela front. *Journal of Experimental Marine Biology and Ecology*, 352, 234–243.

Bachelèlery, M.-L., Illig, S. and Rouault, M. (2019) Interannual coastal trapped waves in the Angola-Benguela upwelling system and Benguela Niño and Niña events. *Journal of Marine Systems*, 203, 103262. https://doi.org/10.1016/j.jmarsys.2019.103262.

Bjerknes, J. (1969) Atmospheric teleconnections from the euqaotrial Pacific. *Monthly Weather Review*, 97, 163–172.

Cabos, W., de la Vara, A. and Koseki, S. (2019) Tropical Atlantic variability: observations and modeling. *Atmosphere*, 10, 502. https://doi.org/10.3309/atmos10090502.

Cai, W., Wu, L., Lengaigne, M., Li, T., McGregor, S., Kug, J.-S., Yu, J.-Y., Stuecker, M.F., Santoso, A., Li, X., Ham, Y.-G., Chikamoto, Y., Ng, B., McPhaden, M.J., Du, Y., Dommenget, D., Jia, F., Kajtar, J.B., Keenlyside, N., Lin, X., Luo, J.-J., Martín-Rey, M., Ruprich-Robert, Y., Wang, G., Xie, S.-P., Yang, Y., Kang, S. M., Choi, J.-Y., Gan, B., Kim, G.-I., Kim, C.-E., Kim, S., Kim, J.-H. & Chang, P. (2019) Pantropical climate interaction. *Science*, 363, eaav4236.

Chavez, F.P. and Messié, M. (2009) A comparison of eastern boundary upwelling ecosystem. *Progress in Oceanography*, 83, 80–96.

Colberg, F. and Reason, C.J.C. (2006) A model study of the Angola Benguela frontal zone: sensitivity to atmospheric forcing. *Geophysical Research Letters*, 33, L19608. https://doi.org/10.1029/2006GL027463.

Copernicus Climate Change Service, 2017. *ERA5: first generation of ECMWF atmospheric reanalyses of the global climate. Copernicus climate change service data store (CDS), data of access.* Available at: http://cds.climate.copernicus.eu/cdsapp#!/home

Dee, D.P., Uppala, S.M., Simmons, A.J., Berrisford, P., Poli, P., Kobayashi, S., Andre, U., Balmaseda, M.A., Balsamo, G., Bauer, P., Bechtold, P., Beljaars, A.C.M., van de Berg, L., Bidlot, J., Bormann, N., Delsol, C., Dragani, R., Fuentes, M., Geer, A.J., Haimberger, L., Healy, S.B., Hersbach, H., Hóml, E. V., Isaksen, L., Kåkkberg, P., Köhler, M., Matricardi, M., McNally, A.P., Monge-Sanz, B.M., Morcrette, J.-J., Park, B.-K., Peubey, C., de Rosnay, P., Tavolato, C., Thépaut, J.-N. and Vitart, F. (2011) The ERA-interim reanalysis: configuration and performance of the data assimilation system. *Quarterly Journal of the Royal Meteorological Society*, 137, 553–597. https://doi.org/10.1002/qj.828.

Dippe, T., Greatbatch, R.J. and Ding, H. (2018) On the relationship between Atlantic Niño and ocean dynamics. *Climate Dynamics*, 51, 597–612. https://doi.org/10.1007/s00382-017-3943-z.

Florenchie, P., Lutejeharms, J.R., Reason, C.J.C., Masson, S. and Rouault, M. (2003) The source of Benguela Niños in the South Atlantic Ocean. *Geophysical Research Letters*, 30(10), 1505. https://doi.org/10.1029/2003GL017171.

Hanshingo, K. and Reason, C.J.C. (2009) Modelling the atmospheric response over southern Africa to SST forcing in the southeast tropical Atlantic and southwest subtropical Indian oceans. *International Journal of Climatology*, 29, 1001–1012. https://doi.org/10.1002/joc.1919.

Hess, G.D. (2004) The neutral, barotropic planetary boundary layer, capped by a low-level inversion. *Boundary-Layer Meteorology*, 110, 319–355.

Illig, S., Cadier, E., Bachèlery, M.-L. and Kersalé, M. (2018) Subseasonal coastal trapped wave propagations in the southeastern Pacifc and Atlantic oceans: 1. A new approach to estimate wave amplitude. *Journal of Geophysical Research, Oceans*, 123(6), 3915–3941. https://doi.org/10.1029/2017/JC013539.

Imbol Koungue, R.A., Illig, S. and Rouault, M. (2017) Role of interannual kelvin wave propagations in the equatorial Atlantic on the Angola Bneguela current system. *Journal of Geophysical Research, Oceans*, 122, 4685–4703. https://doi.org/10.1002/2016JC012463.

Imbol Koungue, R.A., Rouault, M., Illig, S., Brandt, P. and Jouanno, J. (2019) Beguela Niños and Benguela Niñas in Forced Ocean simulation from 1958 to 2015. *Journal of Geophysical Research, Oceans*, 124, 5923–5951. https://doi.org/10.1029/2019/JC015013.

Jarre, A., Hutchings, L., Kirkman, S.P., Kreiner, A., Tchipalanga, P. C.M., Kainge, P., Uanivi, U., van der Plas, A.K., Blamey, L.K., Coetzee, J.C., Lamont, T., Samaai, T., Verheye, H.M., Yamane, D.G., Axelsen, B.E., Ostrowski, M., Stenevik, E.K. and Loeng, H. (2015) Synthesis: climate effects on biodiversity, abundance and distribution of marine organisms in the Benguela. *Fisheries Oceanography*, 24, 122–149. https://doi.org/10.1111/fog.12086.

Jouanno, J., Hernandez, O. and Sanchez-Gomez, E. (2017) Equatorial Atlantic interannual variability and its relation to dynamic and thermodynamic processes. *Earth System Dynamics*, 8, 1061–1069. https://doi.org/10.5194/esd-8-1061-2017.

Junker, T., Schmidt, M. and Mohrholz, V. (2015) The relation of wind stress curl and meridional transport in the Benguela upwelling system. *Journal of Marine Research*, 143, 1–6.

Kataoka, T., Tozuka, T., Behera, S. and Yamagata, T. (2013) On the Nigaloo Niño/Niña. *Climate Dynamics*, 43(5–6), 1463–1482. https://doi.org/10.1007/s00382-013-1961-z.

Kato, S., Rose, F.G., Ham, S.-H., Rutan, D.A., Radkevich, A., Caldwell, T.E., Sun-Mack, S., Miller, W.F. and Chen, Y. (2018) Radiative heating rates computed with clouds derived from satellite-based passive and active sensors and their effects on generation of available potential energy. *Journal of Geophysical Research – Atmospheres*, 124, 1720–1740. https://doi.org/10.1029/2018JD028878.

Keenlyside, N. and Latif, M. (2007) Understanding equatorial Atlantic interannual variability. *Journal of Climate*, 20, 131–142. https://doi.org/10.1175/JCLI3992.1.

Klein, S.A. and Hartmann, D.L. (1993) The seasonal cycle of low Stratiform clouds. *Journal of Climate*, 6, 1587–1606.

Koračin, D., Businger, J.A., Dorman, C.E. and Lewis, J.M. (2005) Formation, evolution, and dissipation of coastal sea fog. *Boundary-Layer Meteorology*, 117, 447–478. https://doi.org/10.1007/s10546-005-2772-5.

Koseki, S., Nakamura, T., Mitsudera, H. and Wang, Y. (2012) Modeling low-level cloud over the Okhotsk Sea in summer: cloud formation and its effect on the Okhotsk high. *Journal of Geophysical Research – Atmospheres*, 117, D05208. https://doi.org/10.1029/2011JD016462.

Koseki, S., Keenlyside, N., Demissie, T., Toniazzo, T., Counillon, F., Bethle, I., Ilicak, M. and Shen, M.-L. (2018) Causes of the large warm bias in the Angola-Benguela frontal zone in the Norwegian earth system model. *Climate Dynamics*, 50(11–12), 4651–4670. https://doi.org/10.1007/s00382-017-3896-2.

Koseki, S., Giordani, H. and Gouvanoba, K. (2019) Frontogenesis of the Angola-Benguela frontal zone. *Ocean Science*, 15, 83–96. https://doi.org/10.5194/os-15-83-2019.

Kopte, R., Brandt, P., Dengler, M., Tchipalanga, P.C.M., Macueria, M. and Ostrowski, M. (2017) The Angola current: flow and hydrographic characteristic as observed at 11°S. *Journal of Geophysical Research, Oceans*, 122, 1177–1189. https://doi.org/10.1002/2016JC012374.

Lima, D.C., Soares, P.M.M., Semedo, A., Cardoso, R.M., Cabos, W. and Sein, D.V. (2019) A climatological analysis of the Benguela coastal low-level jet. *Journal of Geophysical Research – Atmospheres*, 124, 3960–3978.

Lindzen, R. S. & Nigam, S. (1987) On the role of sea surface temperature gradients in forcing low-level winds and convergence in the tropics. *Journal of Atmospheric Science*, 44(17), 2418–2436. https://journals.ametsoc.org/jas/article/44/17/2418/21742/On-the-Role-of-Sea-Surface-Temperature-Gradients.

Lutz, K., Jacobeit, J. and Rathmann, J. (2015) Atlantic warm and cold water events and impact on African west coast precipitation. *International Journal of Climatology*, 35, 128–141. https://doi.org/10.1002/joc.3969.

Lübbecke, J.F., Böning, C.W., Keenlyside, N.S. and Xie, S.-P. (2010) On the connection between Benguela and equatorial Atlantic Niños and the role of the South Atlantic anticyclone. *Journal of Geophysical Research: Oceans*, 115, C09015. https://doi.org/10.1029/2009JC005964.

Manhique, A.J., Reason, C.J.C., Silinto, B., Zucula, J., Raiva, I., Congolo, F. and Mavume, A.F. (2015) Extreme rainfall and floods in southern Africa in January 2013 and associated circulation patterns. *Natural Hazards*, 77, 679–691. https://doi.org/10.1007/s11069-015-1616-y.

Mohrholz, V., Schmidt, M., Lutjeharms, J.R.E. and John, H.-C.H. (2004) Space-time behavior of the Angola-Benguela frontal zone during the Benguela Nino of April 1999. *International Journal of Remote Sensing*, 25, 1400–1340. https://doi.org/10.1080/01431160310001592265.

Neale, R.B., Chen, C.-C. and Gettleman, A. (2010) *Description of the NCAR community atmospheric model (CAM5.0)*. Boulder: NCAR.

Nicholls, S. (1984) The dynamics of stratocumulus: aircraft observations and comparison with a mixed layer model. *Quarterly Journal of the Royal Meteorological Society*, 110, 783–820. https://doi.org/10.1002/qj.49711046603.

Potter, S.F., Dawson, E.J. and Frierson, D.M.W. (2017) South African orography impacts on low clouds and the Atlantic ITCZ in a coupled model. *Geophysical Research Letters*, 44, 3283–3289. https://doi.org/10.1002/2017GL073098.

Rayner, N.A., Parker, D.E., Horton, E.B., Folland, C.K., Alexander, L.V., and Rowell, D.P. (2003) Global analyses of sea surface temperature, sea ice, and night marine air temperature since the late nineteenth century. *Journal of Geophysical Research*, 108(D14), 4407. https://doi.org/10.1029/2002JD002670.

Richter, I. and Mechoso, C.R. (2004) Orographic influences on the annual cycle of Namibian stratocumulus clouds. *Geophysical Research Letters*, 31, L24108. https://doi.org/10.1029/2004GL020814.

Richter, I., Behara, S.K., Masumoto, Y., Taguchi, B., Komori, N. and Yamagata, T. (2010) On the triggering of Benguela Niños: remote equatorial versus local influences. *Geophysical Research Letters*, 37, L20604. https://doi.org/10.1029/2010GL044461.

Rouault, M., Florenchie, P., Fauchereau, N. and Reason, C.J.C. (2003) South east tropical Atlantic warm events and southern African rainfall. *Geophysical Research Letters*, 30, 8009. https://doi.org/10.1029/2002/GL014840.

Rouault, M., Illig, S., Bartholomae, C., Reason, C.J.C. and Bentamy, A. (2007) Propagation and origin of warm anomalies in the Angola Benguela upwelling system in 2001. *Journal of Marine Systems*, 68(3–4), 473–488. https://doi.org/10.1016/j.jmarsys.2006.11.010.

Rouault, M., Illig, S., Lübbecke, J.F. and Koungue, R.A.I. (2018) Origin, development, and demise of the 2010-2011 Benguela Niño. *Journal of Marine Systems*, 188, 39–48. https://doi.org/10-1016/j.jmarsys.2017.07.007.

Schiffer, R.A. and Rossow, W.B. (1983) The international satellite cloud climatology project (ISCCP): the Frist project of the world climate research Programme. *Bulletin of the American Meteorological Society*, 64, 779–784.

Siegfried, L., Schmidt, M., Mohrholz, V., Pogrzeba, H., Nardini, P., Böttinger, M. and Scheuermann, G. (2019) The tropical-subtropical coupling in the Southeast Atlantic from the perspective of the northern Benguela upwelling system. *PLoS One*, 14(1), e0210083. https://doi.org/10.1371/journal.pone.0210083.

Tchipalanga, P., Dengler, M., Brandt, P., Kopte, R., Macuéria, M., Coelho, P., Ostowski, M. and Keenlyside, N. (2018) Eastern boundary circulation and hydrography off Angola: building Angolan oceanographic capacities. *Bulletin of the American Meteorological Society*, 99, 1589–1605. https://doi.org/10.1175/BAMS-D-17-0197.1.

Tokinaga, H., Tanimoto, Y., Nonaka, M., Taguchi, B., Fukamachi, T., Xie, S.-P., Nakamura, H., Watanabe, T. and Yasuda, I. (2006) Atmospheric sounding over the winter Kuroshio extension: effect of surface stability on atmospheric boundary layer structure. *Geophysical Research Letters*, 33, L04703. https://doi.org/10.1029/2005GL025102.

Tokinaga, H. and Xie, S.-P. (2009) Ocean tidal cooling effect on summer sea fog over the Okhotsk Sea. *Journal of Geophysical Research – Atmospheres*, 114, D14102. https://doi.org/10.1029/2008JD011477.

Vizy, E.K., Cook, K.H. and Sun, X. (2018) Decadal change of the South Atlantic Ocean Angola-Benguela frontal zone since 1980. *Climate Dynamics*, 51, 3251–3273. https://doi.org/10.1007/s00382-018-4077-7.

Voldoire, A., Exarchou, E., Sanchez-Gomez, E., Demissie, T., Deppenmeier, A.-L., Frauen, C., Goubanova, K., Hazeleger, W., Keenlyside, N., Koseki, S., Prodhomme, C., Shonk, J., Toniazzo, T. and Traoré, A.-K. (2019) Role of wind stress in driving SST biases in the tropical Atlantic. *Climate Dynamics*, 53(5–6), 3481–3504. https://doi.org/10.1007/s00382-019-04717-0.

Wallace, J., Mitchell, T.P. and Deser, C. (1989) The influence of sea-surface temperature on surface wind in the eastern equatorial Pacific: seasonal and interannual variability. *Journal of Climate*, 2, 1492–1499.

Wood, R. (2012) Stratocumulus clouds. *Monthly Weather Review*, 140, 2373–2423.

Xu, Z., Chang, P., Richter, I., Kim, W. and Tang, G. (2014) Diagnosing south-east tropical Atlantic SST and ocean circulation biases in the CMIP ensemble. *Climate Dynamics*, 43, 3123–3145. https://doi.org/10.1007/s00382-014-2247-9.

SUPPORTING INFORMATION

Additional supporting information may be found online in the Supporting Information section at the end of this article.

How to cite this article: Koseki S, Imbol Koungue RA. Regional atmospheric response to the Benguela Niñas. *Int J Climatol*. 2021;41 (Suppl. 1):E1483–E1497. https://doi.org/10.1002/joc.6782